© 2019. Published by The Company of Biologists Ltd | Journal of Experimental Biology (2019) 222, jeb191791. doi:10.1242/jeb.191791

RESEARCH ARTICLE

Energetics and behavior of coral reef fishes during oscillatory swimming in a simulated wave surge

Travis M. Marcoux and Keith E. Korsmeyer*

ABSTRACT

Oxygen consumption rates were measured for coral reef fishes during swimming in a bidirectional, oscillatory pattern to simulate station-holding in wave-induced, shallow-water flows. For all species examined, increases in wave intensity, as simulated by increases in frequency and amplitude of oscillation, yielded increased metabolic rates and net costs of swimming (NCOS; swimming metabolic rate minus standard metabolic rate). Comparing species with different swimming modes, the caudal fin swimming *Kuhlia* spp. (Kuhliidae) and simultaneous pectoral–caudal fin swimming *Amphiprion ocellaris* (Pomacentridae) turned around to face the direction of swimming most of the time, whereas the median–paired fin (MPF) swimmers, the pectoral fin swimming *Ctenochaetus strigosus* (Acanthuridae) and dorsal–anal fin swimming *Sufflamen bursa* (Balistidae), more frequently swam in reverse for one half of the oscillation to avoid turning. Contrary to expectations, the body–caudal fin (BCF) swimming *Kuhlia* spp. had the lowest overall NCOS in the oscillatory swimming regime compared with the MPF swimmers. However, when examining the effect of increasing frequency of oscillation at similar average velocities, *Kuhlia* spp. showed a 24% increase in NCOS with a 50% increase in direction changes and accelerations. The two strict MPF swimmers had lower increases on average, suggestive of reduced added costs with increasing frequency of direction changes with this swimming mode. Further studies are needed on the costs of unsteady swimming to determine whether these differences can explain the observed prevalence of fishes using the MPF pectoral fin swimming mode in reef habitats exposed to high, wave-surge-induced water flows.

KEY WORDS: Respirometry, Unsteady swimming, Balistiform, Labriform, Wave stress

INTRODUCTION

In coastal habitats, wave-induced water motions result in complex flow characteristics that strongly influence community composition (Denny and Gaylord, 2010). Wave-driven flow regimes are particularly prevalent on fringing and barrier reefs, reducing wave energy before it reaches the coastline (Moberg and Folke, 1999). Contending with wave stress is potentially an energetically expensive endeavor for fishes, and those that are behaviorally, morphologically or physiologically adapted to minimize energy expenditure will have a selective advantage in occupying areas of increased water flows (Fulton et al., 2013b). The intensity of wave exposure has been identified as an important factor affecting reef fish distributions, with correlations with fish morphology and swimming performance (Bellwood and Wainwright, 2001; Fulton, 2010; Webb et al., 2010; Fulton et al., 2017).

Coral reef fishes display a great diversity of body and fin shapes, and also swimming gaits, or patterns of fin use for swimming (Price et al., 2011; Fulton et al., 2013b; Pink and Fulton, 2014). Swimming mode in fishes can be divided into two broad functional groups: body–caudal fin (BCF) swimming, using lateral undulations of the body and caudal fin, and median–paired fin (MPF) swimming, involving movements of one or more median (dorsal and anal) or paired (pectoral) fins, while the body is held rigid (Webb, 1998). In a census of coral reef fishes, Fulton (2007) categorized species into four swimming modes based on fin use observed during routine swimming: caudal (BCF); two categories of MPF swimming, pectoral and dorsal–anal; and an intermediate form, simultaneous pectoral–caudal. BCF (caudal) swimming is the ancestral form of locomotion in fishes and an estimated 85% of all fish families primarily use this mode of propulsion (Lauder and Liem, 1983; Videler, 1993). On coral reefs, however, over 60% of observed species are pectoral fin swimmers, such as wrasses (Labridae), surgeonfishes (Acanthuridae) and many damselfishes (Pomacentridae) (Fulton and Bellwood, 2005; Fulton et al., 2017). Net water flows are highest on wave-exposed and shallow areas of the reef crest and flats, and the prevalence of pectoral fin swimmers increases as a function of habitat water velocities, whereas the BCF swimmers, both caudal and pectoral–caudal, show the opposite trend (Fulton and Bellwood, 2005). These trends suggest that the pectoral fin, MPF swimming mode is particularly well adapted for areas of increased wave-driven water flows. BCF swimming is generally considered most effective for fast, steady swimming and rapid accelerations (Webb, 1984; Blake, 2004); however, some MPF swimmers are also capable of high, steady swimming speeds (Korsmeyer et al., 2002; Walker and Westneat, 2002; Fulton, 2007; Fulton et al., 2013a). Studies of the energetic costs of pectoral fin swimming suggest that some species are adapted for efficient, sustained, high-speed swimming, which could be an adaptation to living in habitats with high water flows (Webb, 1974; Korsmeyer et al., 2002; Fulton et al., 2013a). Yet there is a general hypothesized trade-off between steady (constant speed, straight line) and unsteady swimming activities (Langerhans, 2008; Langerhans and Reznick, 2010). For a particular swimming mode, traits linked to increased performance during steady and high-speed swimming are thought to decrease unsteady performance (e.g. maneuverability, stability at low speeds) and vice versa (Webb, 1994; Drucker and Lauder, 2000; Walker and Westneat, 2002; Blake, 2004; Domenici, 2010). Although the ability to swim efficiently at high steady speeds may be beneficial in the reef habitats with high net water velocities, owing to the nature of wave-driven shallow-water flows, fishes in these areas must also effectively maneuver and adjust to maintain position and stability.

Department of Natural Sciences, Hawaii Pacific University, 1 Aloha Tower Drive, Honolulu, HI 96813, USA.

*Author for correspondence (kkorsmeyer@hpu.edu)

K.E.K., 0000-0003-4457-3495

Received 4 September 2018; Accepted 11 January 2019

Journal of Experimental Biology (2019) 222, jeb191791. doi:10.1242/jeb.191791

As wind-driven waves travel inshore and water depth decreases over shallow reefs (depth less than one-half wavelength), the circular, wave-induced water movement is compressed into a predominantly longitudinal, or horizontal, motion known as wave surge, characterized by bidirectional, oscillatory water flow (Fulton and Bellwood, 2005; Denny, 2006; Constantin and Villari, 2008; Webb et al., 2010). Fishes that occupy shallow coral reefs must cope with constant changes in water velocity and direction. Holding station on the reef, to maintain access to forage area or territory, for example, requires changes in direction and accelerations with each passing wave surge, which would be expected to increase energetic costs (Webb et al., 2010; Heatwole and Fulton, 2013). Most studies on fish swimming have examined the energetics and performance of steady, straight-line swimming (Korsmeyer et al., 2002; Fulton et al., 2005, 2013a; Svendsen et al., 2010); however, no studies have investigated energetics of fishes while swimming in water with periodic changes in velocity and direction, which are typical of flows on wave-swept reefs.

In this study, we examined the energetic costs and swimming behaviors during bidirectional, oscillatory swimming in fish species encompassing four different modes of locomotion in reef fishes: caudal, pectoral–caudal, pectoral and dorsal–anal fin swimming (Fulton, 2007). Using a novel apparatus, the simulated wave motion respirometer (SWMR), we measured the relationship between swimming mode and energetic costs in fish swimming in an increasing regime of simulated wave surge intensities. By testing species with different swimming modes, we intended to discern which swimming strategies might provide a selective advantage in occupying areas of increased wave-driven water flows.

MATERIALS AND METHODS

Fish acquisition

Species were selected based on availability and to cover a range of swimming modes (Table 1). Primary swimming mode was determined by observations during the swimming experiment. The caudal fin swimmers included the Hawaiian flagtail, *Kuhlia xenura* (Jordan and Gilbert 1882), and reticulated flagtail, *Kuhlia sandvicensis* (Steindachner 1876). Because distinguishing between *K. xenura* and *K. sandvicensis* was uncertain at the sizes used for this study, the species are referred to as the complex, *Kuhlia* spp. (Randall and Randall, 2001). Five specimens were used in the swimming experiments (Table 1) and one additional, larger individual (16.7 g) was included for determination of standard metabolic rate (SMR) to help resolve the metabolic scaling exponent. The *Kuhlia* spp. were collected with beach seines from nearshore Oahu. The clown anemonefish, *Amphiprion ocellaris* Cuvier 1830, is a simultaneous pectoral–caudal fin swimmer, and individuals were obtained from captive-bred stocks at the Oceanic Institute of Hawaii Pacific University, Waimanalo, HI, USA. The goldring surgeonfish, *Ctenochaetus strigosus* (Bennett 1828), is primarily a pectoral fin swimmer and the lei triggerfish, *Sufflamen bursa* (Bloch and Schneider 1801), is a dorsal–anal fin swimmer. These latter two species were obtained from local wholesale aquarium fish retailers.

All subjects were held in flow-through seawater tanks (26–28°C, S=30–32, 12 h:12 h light:dark photoperiod) at the Oceanic Institute of Hawaii Pacific University and fed daily with commercial marine fish pellets and chopped frozen squid. Fish were acclimated in laboratory conditions for at least two weeks before testing. All fish were handled ethically according to Hawaii Pacific University's Institutional Animal Care and Use Policies.

Simulated wave motion respirometer

The challenges of measuring oxygen consumption rates in fish in wave-swept oscillatory flows have prevented prior energetic studies under these conditions. Respirometry requires a closed chamber to prevent oxygen diffusion from an air–water interface, or outside volumes of water, making wave tanks unsuitable (Fish and Hoffman, 2015). In addition, accurate measurements of oxygen consumption require a low water volume to fish mass ratio, while still providing sufficient space for unobstructed movements of the fish (Clark et al., 2013). To solve these technical issues, the simulated wave motion respirometer (SWMR) was developed to take oxygen consumption measurements while replicating station-holding swimming behavior against a bidirectional wave surge (Fig. 1). A traditional swim flume for studies of fish swimming creates steady, unidirectional flows and the fish swims in place to simulate a fish swimming through still water (Tudorache et al., 2013). The SWMR uses the corollary to this method, by having the fish swim back and forth in still water to simulate swimming in place against wave-driven oscillatory flows (wave orbits>>fish length) (Vogel, 1994). The SWMR shifts the frame of reference to the surrounding water mass, rather than the seafloor, and utilizes the optomotor response for rheotaxis in fish to induce oscillatory swimming within the respirometer (Harden Jones, 1963; Arnold, 1974). The SWMR allowed repeatable measurements of oscillatory swimming under controlled frequencies and amplitudes in a limited volume of water suitable for respirometry.

Oscillatory swimming movements were induced by placing the fish in a 15-cm-long swimming shuttle that travels back and forth inside a 50-cm-long clear acrylic respirometry tube (8.9 cm inside diameter; Fig. 1). The swimming shuttle was composed of two PVC rings with a plastic screen at either end that were magnetically coupled through the walls of the respirometer to an external sleeve. The external sleeve slid along the respirometry tube, conveyed by a Scotch yoke, or slotted link, mechanism to convert rotation, driven by an electric motor with variable speed control, to linear, sinusoidal motion. Adjustments of the motor rotation speed and radius of the rotation were used to alter the wave frequency and amplitude, respectively, of the simulated wave surge (Fig. 1C). The external sleeve was marked with black and white vertical bars to serve as a strong visual reference to elicit the optomotor response and induce swimming to follow the moving section. The movement of the background visual field simulated displacement by a current, and the fish oriented to the perceived flow and swam to maintain position relative to visual cues

Table 1. Species, primary swimming mode, sample size (*N*), mean mass and body length (range), and mass-specific standard metabolic rates (SMR, mean [95% confidence interval])

Species	Primary swimming mode	*N*	Mass (g)	Body length (cm)	SMR (mg O_2 kg^{-1} h^{-1})	SMR_{10}* (mg O_2 kg^{-1} h^{-1})
Kuhlia xenura/*K. sandvicensis*	Caudal	5	5.5 (3.9–8.8)	7.4 (6.5–8.8)	158 [98, 218]	148 [85, 212]
Amphiprion ocellaris	Pectoral–caudal	5	5.3 (4.5–6.3)	6.5 (6.0–6.9)	144 [98, 190]	135 [92, 177]
Ctenochaetus strigosus	Pectoral	6	8.9 (7.9–10.1)	7.5 (7.1–8.2)	172 [136, 209]	170 [134, 207]
Sufflamen bursa	Dorsal–anal	5	9.2 (6.4–12.3)	7.4 (7.0–8.0)	107 [70, 145]	106 [70, 142]

*SMR_{10} values are mass-specific SMRs adjusted to a common mass of 10 g using a mass scaling exponent of 0.895.

Journal of Experimental Biology (2019) 222, jeb191791. doi:10.1242/jeb.191791

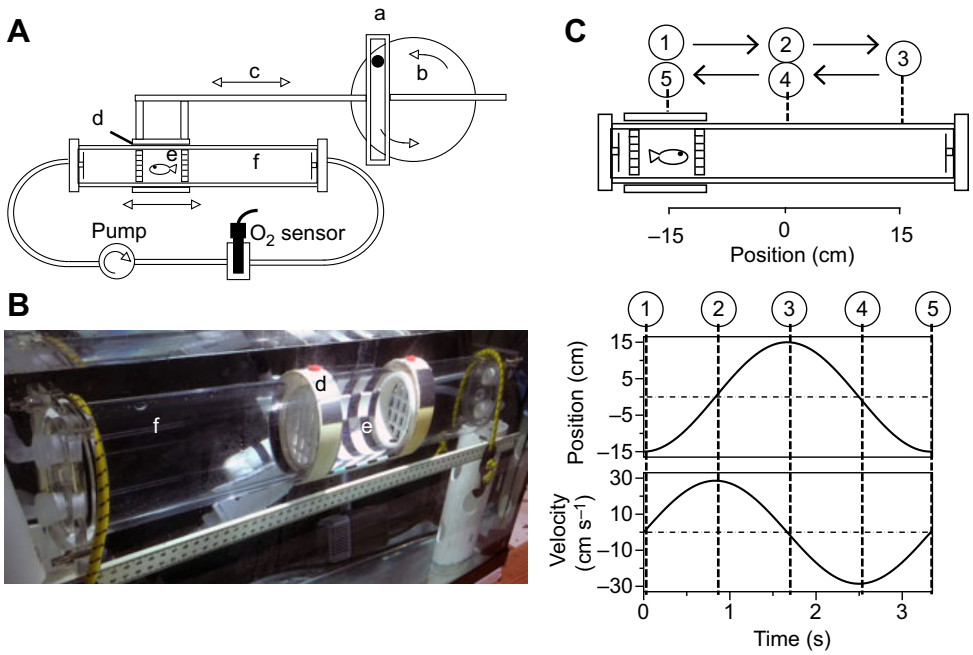

Fig. 1. The simulated wave motion respirometer (SWMR). (A) Schematic of the SWMR apparatus. A Scotch yoke mechanism (a) is used to convert rotational motion (b) into linear oscillation (c), with sinusoidal displacement and velocity over time. A partial sleeve (d), surrounding a long (50 cm) cylindrical (8.9 cm inner diameter) clear acrylic respirometry tube (f), is coupled to internal PVC rings by magnets, creating a 15-cm-long swimming shuttle (e) that travels back and forth within the respirometer. Water within the respirometer tube is circulated past an optical dissolved oxygen sensor for measurement of oxygen consumption rate. A second computer-actuated pump (not shown) periodically flushes the respirometer with clean oxygenated water from a surrounding water bath. (B) Photo of respirometer tube (f) with sleeve (d) and swimming shuttle (e) submerged in a glass aquarium. (C) Example of movement and velocity of swimming shuttle during a single oscillation at 0.3 Hz (period=3.3 s) and an amplitude of 15 cm. Positions in respirometer tube (1–5) are shown (top), as well as the corresponding horizontal position and velocity over time (bottom). By changing the rotational speed and radius of the circular motion, the wave frequency and amplitude, respectively, can be altered.

(Arnold, 1974). From the fish's perspective, it was swimming against a water current to hold station, relative to the swimming shuttle. The view into the swimming shuttle was unobstructed from one side to allow video recordings. In addition, an LED lamp was attached above the swimming shuttle and to the sliding mechanism, so that it followed the movements to provide consistent illumination from above. This both provided lighting for the video recordings and prevented changing shadows as the swimming section moved. A blind of uniform color to prevent contradictory visual cues surrounded the entire apparatus. A small video camera (GoPro) was attached to the sliding arm to move with the swimming shuttle and provide a stable video image relative to the shuttle. Particle tracking experiments confirmed repeatable relative water movements, following the expected waveform with minimal turbulence (Fig. S1; Meijering et al., 2012; Roche et al., 2014).

The SWMR respirometer (volume=3.15 liters) was submerged in a flow-through (~2 l min^{-1}) seawater bath (110 liter glass aquarium; Fig. 1B) to maintain consistent temperature (26±1°C). Oxygen consumption rates were measured using computerized, intermittent-flow respirometry (Svendsen et al., 2016). A closed loop of tubing with a submersible pump circulated water through the swimming chamber and past an optical dissolved oxygen sensor and conductivity probe for continuous measurement of oxygen content, temperature and salinity. A second, computer-actuated, submersible pump was used to initiate the flushing phase of the intermittent-flow respirometry cycle and pump aerated seawater from the surrounding tank through the respirometer. Water in the seawater bath was continuously pumped through an ultraviolet sterilizer (SmartUV Lite, Emperor Aquatics, Inc.) to reduce background levels of microbial respiration. All probes were calibrated before experimentation according to manufacturer specifications and were connected to an Orion 5-Star Portable pH/ORP/ISE/DO/Conductivity Multimeter (Thermo Fisher Scientific, Waltham, MA, USA) that automatically corrects dissolved oxygen content for the temperature and salinity of the water. Output from the multimeter was sent to a computer for continuous recording (0.2 Hz) via LabView 2014 (National Instruments, Austin, TX, USA).

Experimental procedure

Before conducting each experiment, oxygen consumption rates were recorded for 1 h to determine the initial background level of microbial oxygen consumption in the SWMR apparatus without a subject. Each respirometry measurement cycle was 12 min in duration, with a 4 min open flushing phase, a 1 min closed mixing phase and a 7 min closed recirculation phase during which the decline in oxygen content was measured. Subjects were fasted for 36 h prior to testing to prevent elevated metabolic rates associated with digestion. Each subject was measured for total body length (BL) and mass, and then placed into the SWMR and allowed to acclimate overnight for at least 18 h. During this period, oxygen consumption rate was recorded to determine the SMR. Following overnight acclimation, the fish were run through an exercise regime of increasing amplitudes of oscillatory swimming at 10, 5 and 3.3 s wave periods (frequencies of 0.1, 0.2 and 0.3 Hz, respectively). At each wave frequency, amplitudes of 1.0, 1.5 and up to 2.0 BL were tested with oxygen consumption measured over two 12-min respirometry cycles at each intensity. After the fish was removed from the SWMR, a second 1 h blank procedure was run to determine background levels of microbial oxygen consumption post-experiment.

Frequencies were determined by recording the time required for one complete rotation of the Scotch yoke mechanism (one total oscillation or wave period, T) using a stopwatch (average of five measurements). Frequency (f) was calculated as:

$$f = \frac{1}{T}. \quad (1)$$

Amplitude (A) was determined by adjusting the length of the radius of the Scotch yoke mechanism relative to the length of the subject fish. The peak swimming velocity (U_{peak}) for each combination of wave frequency and amplitude was calculated as:

$$U_{peak} = 2\pi Af. \quad (2)$$

Average swimming velocity ($U_{average}$) was calculated as the mean absolute velocity through one complete sine wave cycle, using the equation:

$$U_{average} = 4Af. \quad (3)$$

Swimming kinematics

Video recordings (GoPro Hero 3+ Black; 1280 × 720 pixels, 120 frames s^{-1}) were used to examine the fin beat frequency (f_{FB}) and percent turning during oscillatory swimming. f_{FB} was measured from a 1 min video recording captured during each 7 min measuring phase. Owing to the lateral view and translucence of the fins in some species, f_{FB} could only be determined for the pectoral fins of *A. ocellaris* and *C. strigosus*.

f_{FB} was calculated as the time required for one full fin beat, starting from the onset of the fin deflection. For each swimming intensity, f_{FB} was calculated over at least three full wave oscillations and separately analyzed for each half of the oscillation, separating out the effect of some fish swimming backwards during one half of the cycle. To analyze changes in f_{FB} over time during half the cycle (from zero velocity to maximum and back to zero velocity), beat-to-beat f_{FB} were combined into time bins (~10) over each half cycle at each frequency and amplitude to allow for direct comparisons at the same relative time point within the cycle (0.6 s bins at 0.1 Hz, 0.3 s at 0.2 Hz, and 0.2 s at 0.3 Hz frequency). f_{FB} for each time bin was calculated separately for individual fish within that intensity (each swimming direction done separately) and averaged together for the mean f_{FB} for each species. Also, from the video recordings, the percent turning with direction change was quantified as the ratio of the number of times the individual turned around relative to the number of changes in direction by the SWMR shuttle.

Determining metabolic rates and net cost of swimming

Oxygen consumption rate ($\dot{M}_{O_2}$) was used as an indirect measure of aerobic metabolic rate and was calculated from the decline in oxygen content during each 7 min closed recirculating phase of the intermittent-flow respirometry cycle. $\dot{M}_{O_2}$ was calculated from the slope of a linear regression fit to the decrease in oxygen content over time using the formula:

$$\dot{M}_{O_2} = sV_{resp}, \quad (4)$$

where s equals the slope of the best-fit linear regression and V_{resp} is the volume of water in the respirometer taking the volume displaced by the fish into account (with the assumption that 1 g of fish equals 1 ml). Metabolic rates were corrected for background respiration assuming a linear change between the two blank measurements before and after experimental measurements.

SMRs were calculated from a frequency histogram of $\dot{M}_{O_2}$ measured overnight, excluding the initial acclimation period (6 h) after placing the fish in the respirometer. Two normal curves were fit to the frequency histogram to separate the lower SMR distribution of $\dot{M}_{O_2}$ from the higher $\dot{M}_{O_2}$ values owing to spontaneous activity (Steffensen et al., 1994; Chabot et al., 2016). The mean of the lower distribution was considered to be the SMR ($\dot{M}_{O_2}$ at rest) for that individual. Net cost of swimming (NCOS) was calculated as the $\dot{M}_{O_2}$ while swimming minus the SMR, making the NCOS the increase in metabolic rate owing to swimming activity of that individual at each intensity (Korsmeyer et al., 2002). For each individual, NCOS was averaged for both cycles run at each swimming intensity. Any cycles where atypical swimming patterns were recorded (e.g. in contact with walls or bottom, erratic movements) were excluded from analysis.

The relationship between total SMR and body mass (M) was examined to correct mass-scaling effects. Mass-specific metabolic rates (MR) were adjusted to a common mass of 10 g using the following equation:

$$MR_{10} = MR_m \times \left(\frac{10}{M}\right)^{b-1}, \quad (5)$$

where MR_m is metabolic rate of fish with body mass M and b is the mass-scaling exponent determined empirically from SMR measurements. The resulting metabolic rates are referred to as SMR_{10} (mass-adjusted standard metabolic rate) and $NCOS_{10}$ (mass-adjusted net cost of swimming).

Statistical analyses

To examine the effect of amplitude and frequency on average f_{FB}, a three-way repeated measures ANOVA was conducted on *A. ocellaris* swimming forward and *C. strigosus* swimming forward and in reverse. A two-way repeated measures ANOVA was used to compare the effect of time and direction of swimming (forward, reverse) on beat-to-beat f_{FB} for *C. strigosus*. Mauchly's test of sphericity was used to test for violations of assumption of sphericity. In those instances, the Greenhouse–Geisser correction was used.

A one-way analysis of covariance (ANCOVA) was conducted on log-transformed total SMR (mg O_2 h^{-1}) with log of mass as the covariate to test for significant differences among species and mass-scaling exponents. To examine the effects of species, frequency and amplitude on $NCOS_{10}$, a marginal linear model was used, using the linear mixed model procedures in SPSS (West et al., 2014). $NCOS_{10}$ was log transformed to improve normality, and the fixed factors were species, frequency, amplitude and frequency×amplitude. Both frequency and amplitude were modeled as continuous variables, and the data were centered by subtracting the means (f=0.2 Hz, A=1.5 BL). A marginal model was set up with repeated measures for frequency and amplitude, and subjects as fish identity. The chosen covariance structure was first-order autoregressive [AR(1)] with heterogeneous variances, based on comparisons of multiple covariance models to find the lowest value of Akaike's information criterion (AIC).

To examine the effect of increasing rates of direction change on $NCOS_{10}$, we compared NCOS at different frequencies, but similar average velocities within species. Different combinations of wave frequency and amplitude can produce the same velocities (Eqn 3; e.g. a lower frequency, higher amplitude oscillation compared with a higher frequency, lower amplitude oscillation). At a higher frequency, but the same velocities, the fish must cope with greater rates of change in velocity (i.e. acceleration) and more frequent flow

Journal of Experimental Biology (2019) 222, jeb191791. doi:10.1242/jeb.191791

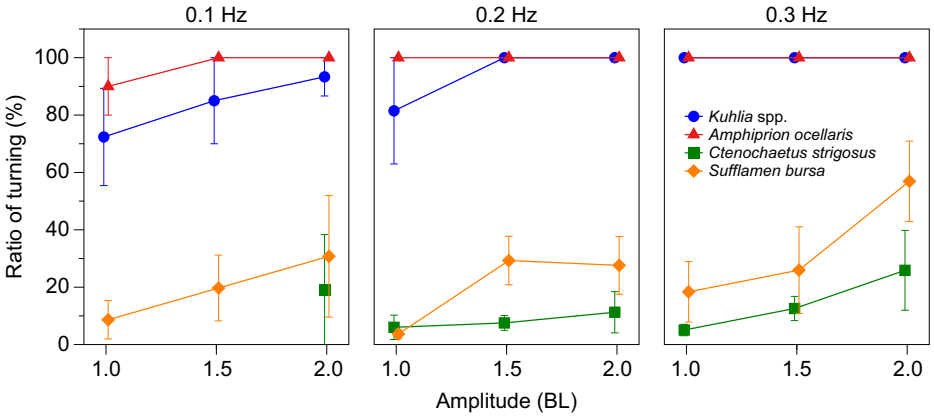

Fig. 2. Ratio of turning to swimming direction changes (mean±s.e.m.) as a function of amplitude at three frequencies, 0.1, 0.2 and 0.3 Hz, during oscillatory swimming. Percent turning was quantified as the number of times the individual turned around relative to the total number of direction changes by the SWMR. Samples sizes are as follows: *Kuhlia* spp., *n*=5; *Amphiprion ocellaris*, *n*=5; *Ctenochaetus strigosus*, *n*=6; and *Sufflamen bursa*, *n*=5. No data exist for *C. strigosus* at the two lowest intensities [0.1 Hz frequency at 1 and 1.5 body length (BL) amplitude] owing to erratic swimming at those wave intensities.

direction changes. Prior to conducting one-way ANCOVA, $NCOS_{10}$ and average velocity were log transformed to linearize the relationship (Korsmeyer et al., 2002). The difference between each log NCOS measurement and the average log NCOS was calculated for each individual as a way to account for the repeated measures design and only examine changes in NCOS. The ANCOVAs were conducted for each species on this difference in log $NCOS_{10}$ from the mean, comparing the 0.2 and 0.3 Hz frequencies, with log average velocity as a covariate.

P-values were adjusted for multiple testing using the Holm–Bonferroni method. Confidence intervals (CI) are reported at the 95% level. Statistical significance level for this study was $P<0.05$ and all tests were conducted with SPSS (IBM, v.25).

RESULTS

Changing swimming direction

All fish species were observed to anticipate the shuttle direction changes after a short period of time, but some fish turned around to maintain forward swimming, while others swam backwards in one direction and forwards in the other (i.e. no turning; Movie 1). Owing to erratic swimming in most of the *C. strigosus* individuals at the lowest two swimming intensities (0.1 Hz at 1.0 and 1.5 BL amplitude), these results were not included in the analyses for this species. *Amphiprion ocellaris* showed the highest percent turning over all amplitudes and frequencies, turning 100% of the time above the lowest wave intensity, followed by *Kuhlia* spp., which turned at least 75% of the time on average and 100% of the time above 0.2 Hz and 1.0 BL amplitude (Fig. 2). Conversely, *C. strigosus* and *S. bursa* typically did not turn around but swam backwards in one direction. As wave intensity increased, *S. bursa* increased the frequency of turning to 55% of the time on average at the highest swimming intensity (Fig. 2). *Ctenochaetus strigosus* turned the least at every intensity compared with all other species, turning less than 30% of the time on average, even at the highest wave intensity.

Pectoral fin-beat frequency

Amphiprion ocellaris swam using a combination of the pectoral fins and body–caudal fin undulations, whereas *C. strigosus* used the pectoral fins almost exclusively. Only pectoral f_{FB} could be reliably measured from the video recordings. Mean f_{FB} increased with both

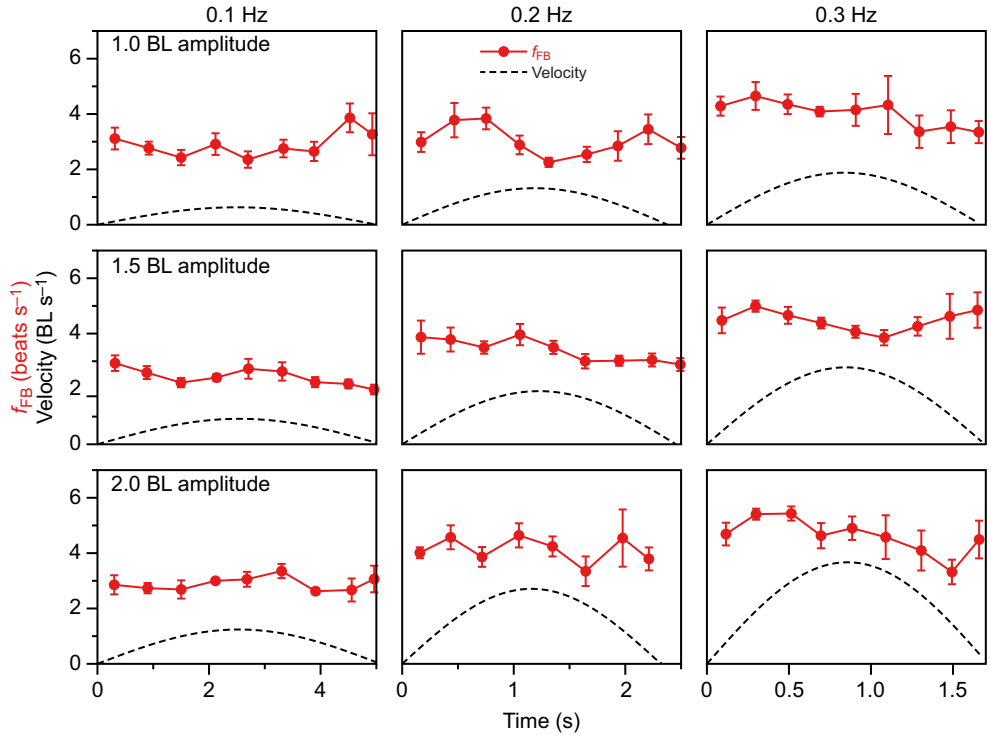

Fig. 3. Pectoral fin-beat frequency (f_{FB}; mean±s.e.m.) as a function of time during one half-cycle of oscillatory swimming for the pectoral–caudal fin swimming clown anemonefish (*Amphiprion ocellaris*). Wave amplitude increases from 1 body length (BL; top row) to 1.5 BL (center row) and 2 BL (bottom row). Wave frequency increases from 0.1 Hz (left column) to 0.2 Hz (center column) and 0.3 Hz (right column). The dashed line indicates the instantaneous velocity of swimming (BL s^{-1}) over time at each wave intensity. *n*=5.

Journal of Experimental Biology (2019) 222, jeb191791. doi:10.1242/jeb.191791

amplitude and frequency ($F_{2,24}$=4.54, P<0.001; $F_{1,12}$=6.15, P<0.001, respectively). For *A. ocellaris*, average pectoral f_{FB} increased from 2.4 to 4.6 beats s^{-1} as swimming intensity increased, and beat-to-beat f_{FB} remained relatively stable throughout each wave cycle (Fig. 3). For *C. strigosus*, average pectoral f_{FB} ranged from 2.8 to 4.8 beats s^{-1} (Fig. 4). However, at all intensities analyzed for *C. strigosus*, f_{FB} varied over time during the oscillation in velocity, while swimming both forwards and in reverse (P<0.05). A common trend was an elevated f_{FB} at the beginning of the cycle (during the period of acceleration as velocity was increasing), followed by a decrease (as velocity peaked and began to decrease), then an abrupt increase nearing the end of the cycle (prior to direction change) (Fig. 4).

At all intensities except for the lowest (f=0.1 Hz, A=2 BL), beat-to-beat f_{FB} in *C. strigosus* was higher when swimming backwards compared with forwards (by 0.5 to 1.2 beats s^{-1} on average). At the two highest intensities, 0.3 Hz frequency and 1.5 and 2 BL amplitude, swimming forward and in reverse affected fin-beat frequency differently over time (ANOVA, interaction between direction and time, $F_{5,20}$=3.12, P=0.030; $F_{4,16}$=4.28, P=0.015, respectively). During backwards swimming, f_{FB} was higher at the beginning of each cycle, but showed a greater decrease in the second half of the cycle, compared with f_{FB} during forward swimming (Fig. 4).

Standard metabolic rate

Overall, the log of mass was related to the log of total SMR with a scaling exponent of 0.895 (ANCOVA, $F_{1,17}$=16.5, P=0.001, r^2=0.56), and was not significantly different across species (ANCOVA, homogeneity of slopes, $F_{3,14}$=0.543, P=0.66). To correct for the small mass differences among individuals, the interspecific mass-scaling exponent was used to normalize all values to a common mass of 10 g. After mass differences were taken into account, average SMR was highest in *C. strigosus* and lowest in *S. bursa*, but with large variances (ANCOVA, $F_{3,17}$=1.90, P=0.17; Table 1).

Net cost of swimming

To remove the effect of individual differences in SMR_{10}, the NCOS ($NCOS_{10}$=swimming MR_{10}–SMR_{10}) was calculated for each swimming intensity, representing the metabolic increment above rest owing to swimming activity. In general, metabolic rates during oscillatory swimming increased with increases in wave amplitude and frequency and also with the average swimming velocity (Fig. 5). The log $NCOS_{10}$ responded differently to increases in amplitude at the different frequencies (significant interaction effect between frequency and amplitude, $F_{1,57.5}$=21.9, P<0.001; Table 2). In general, $NCOS_{10}$ showed greater increases with frequency at higher amplitudes of oscillation and vice versa (Fig. 5). In addition, species had a significant effect on log $NCOS_{10}$ (marginal effect of species pooled over frequency×amplitude, $F_{3,34.1}$=8.53, P<0.001). *Kuhlia* spp. were found to have a lower $NCOS_{10}$ than the other three species at the reference levels of f=0.2 Hz and A=1.5 BL (*post hoc* tests on marginal means; *A. ocellaris*, difference=+104 mg O_2 kg^{-1} h^{-1}, CI[+49, +175], P<0.001; *S. bursa*, difference=+93.8 mg O_2 kg^{-1} h^{-1}, CI[+41.4, +163], P<0.001; *C. strigosus*, difference=+60.9 mg O_2 kg^{-1} h^{-1}, CI[+17.6, +117], P=0.016; Table 2).

The effect of changing direction on swimming costs within species was examined by comparing the change in $NCOS_{10}$ at different frequencies, but at amplitudes that resulted in similar average swimming velocities, which occurred within the 0.2 to 0.3 Hz wave intensities. The rates of increase in $NCOS_{10}$ with average velocity were similar between 0.2 and 0.3 Hz oscillation in three of the four species (ANCOVA homogeneity of slopes, *Kuhlia* spp.: $F_{1,26}$=0.66, P=0.42; *A. ocellaris*: $F_{1,26}$=0.06, P=0.82; *S. bursa*: $F_{1,25}$=1.39, P=0.25; Fig. 6). For *C. strigosus*, however, the slopes were significantly different for the two frequencies ($F_{1,31}$=4.32, P=0.046), with the regression lines intersecting within the range of overlapping velocities (Fig. 6C). On average, *Kuhlia* spp. showed the largest increase in $NCOS_{10}$, with an increase in frequency from 0.2 to 0.3 Hz at similar average velocities

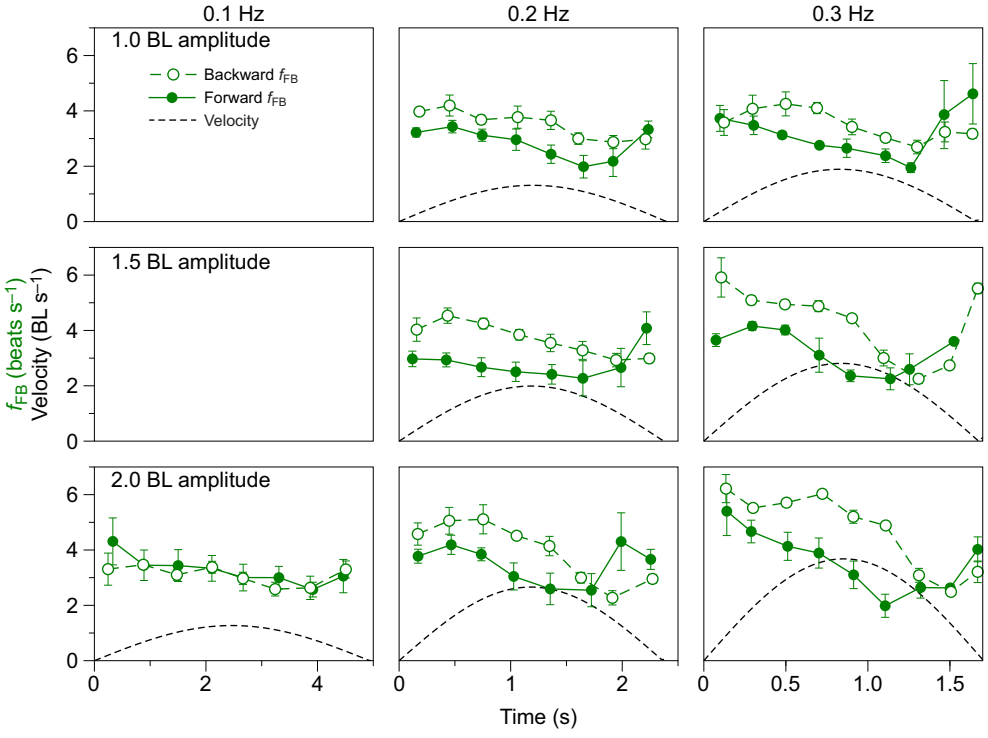

Fig. 4. Pectoral f_{FB} (mean±s.e.m.) as a function of time during one half cycle of oscillatory swimming for the pectoral fin swimming goldring surgeonfish (*Ctenochaetus strigosus*), for both forward swimming (solid symbol) and swimming in reverse (open symbol). Wave amplitude increases from 1 BL (top row) to 1.5 BL (center row) and 2 BL (bottom row). Wave frequency increases from 0.1 Hz (left column), to 0.2 Hz (center column), to 0.3 Hz (right column). The dashed line indicates the instantaneous velocity of swimming (BL s^{-1}) over time at each wave intensity. n=6. No data exist at the two lowest intensities (0.1 Hz frequency at 1 and 1.5 BL amplitude) owing to erratic swimming at those wave intensities.

Journal of Experimental Biology (2019) 222, jeb191791. doi:10.1242/jeb.191791

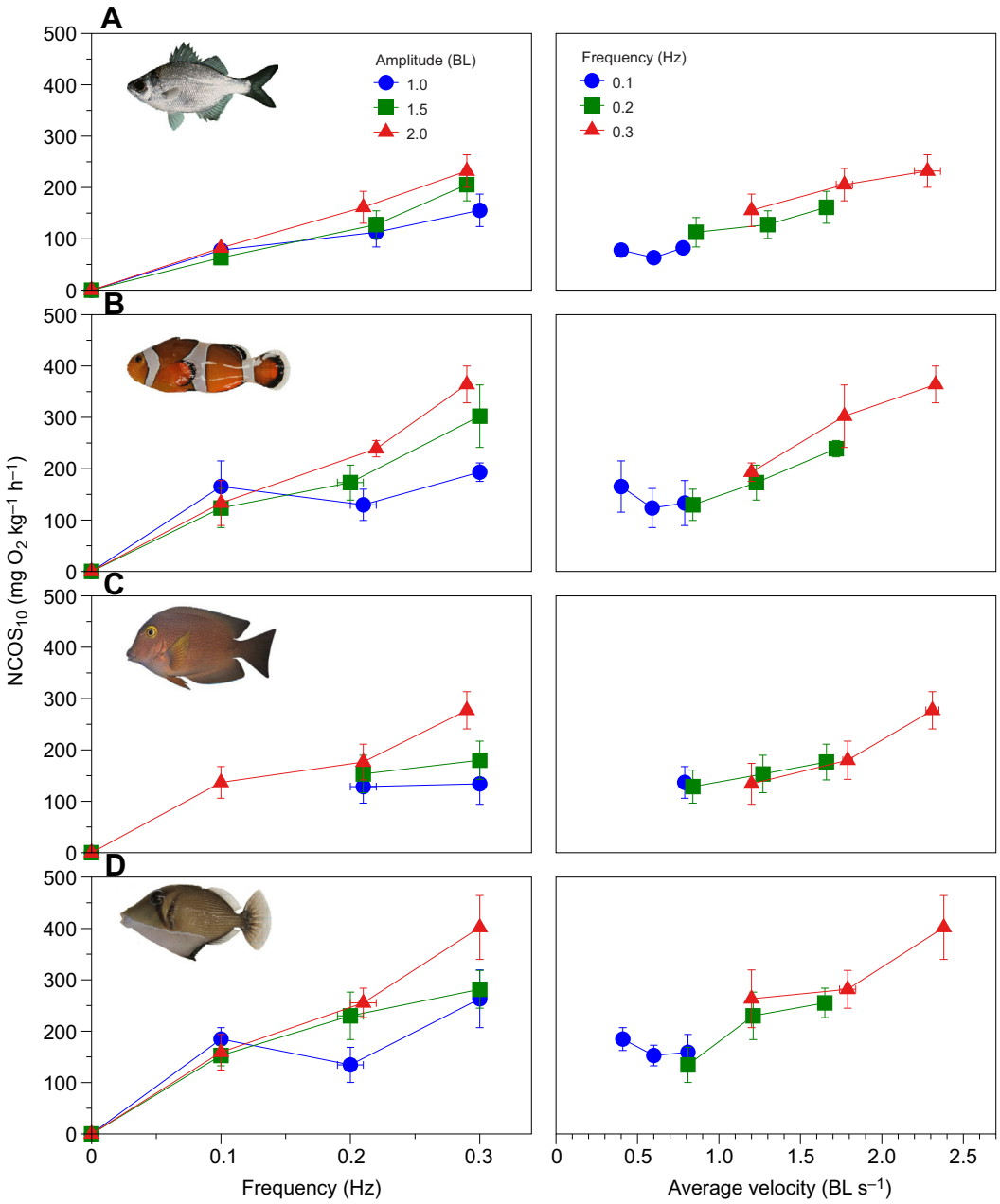

Fig. 5. Net cost of swimming normalized to a common mass of 10 g ($NCOS_{10}$, mean±s.e.m.) as a function of wave frequency (Hz) at three different wave amplitudes (BL; left column), and as a function of average swimming velocity (BL s^{-1}) at the three frequencies (right column), during bidirectional, oscillatory swimming. (A) *Kuhlia* spp. (*n*=5), (B) *Amphiprion ocellaris* (*n*=5), (C) *Ctenochaetus strigosus* (*n*=6) and (D) *Sufflamen bursa* (*n*=5). NCOS was calculated by subtracting SMR from swimming metabolic rate. Average swimming velocity was calculated as the average absolute velocity over one wave cycle. No data exist for *C. strigosus* at the two lowest intensities (0.1 Hz frequency at 1 and 1.5 BL amplitude) owing to erratic swimming at those wave intensities.

(difference=+24%; CI[+7, +43]; *P*=0.006), indicating higher net swimming costs owing to the increases in frequency of direction change, regardless of average swimming velocity (Fig. 6A). *Amphiprion ocellaris* had a smaller average difference in $NCOS_{10}$ (+17%; CI[–2, +39]; *P*=0.084), followed by *S. bursa* (+13%; CI[–5, +34]; *P*=0.16; Fig. 6B,D). For *C. strigosus*, simple main-effects tests were conducted that allow for heterogeneity of slopes to assess differences between frequencies over the range of overlapping velocities (log velocities in BL s^{-1} of 0.10, the mean of 0.164, and 0.25). The simple main-effects tests were not significant (*P*>0.29) and $NCOS_{10}$ was very similar at both frequencies at the same average velocities for *C. strigosus* (difference at mean velocity=−3%, CI[–25, +27]; *P*=0.83; Fig. 6C). Comparing the two groups that differed most in the effect of frequency on $NCOS_{10}$, the *Kuhlia* spp. average response was 27 percentage points higher than in *C. strigosus*, but with wide 95% confidence limits (CI[–11, +81], *P*=0.16).

DISCUSSION

This study examined the energetic costs for fishes swimming against wave-driven oscillations in flow direction to remain in position above the ocean floor (i.e. station-holding). By inducing rheotaxis in a modified respirometer (SWMR; Fig. 1), we were able to induce swimming at wave periods (3.3–10 s) and velocities

Journal of Experimental Biology (2019) 222, jeb191791. doi:10.1242/jeb.191791

Table 2. Estimates of fixed effects from a marginal linear model of log $NCOS_{10}$

Variables	Coefficient	95% confidence limits	*P*-value
Intercept	2.06	[1.96, 2.17]	<0.001
Species			
A. ocellaris	0.273	[0.151, 0.396]	<0.001
S. bursa	0.253	[0.130, 0.375]	<0.001
C. strigosus	0.180	[0.060, 0.299]	0.004
f	1.13	[0.734, 1.53]	<0.001
A	0.139	[0.097, 0.181]	<0.001
f×*A*	1.23	[0.744, 1.86]	<0.001

Frequency (*f*) and amplitude (*A*) of wave motion were modeled as repeated measures, and were centered at *f*=0.20 Hz and *A*=1.5 BL. The reference group for species was *Kuhlia* spp. $logNCOS_{10}$, log-transformed net cost of swimming (mg O_2 kg^{-1} h^{-1}) normalized to a body mass of 10 g.

(0–29 cm s^{-1}) within the range of flows measured on coral reefs (Fulton and Bellwood, 2005; Lowe et al., 2005; Denny, 2006; Madin et al., 2006; Clarke et al., 2009). The metabolic rate of fishes swimming in this oscillatory pattern of wave surge was found to increase as both frequency and amplitude of wave action increased, indicating higher metabolic costs to station-hold as wave action increases (Fig. 5). For fishes living in coastal, wave-swept areas, many strategies exist to cope with increases in wave action, including seeking refuge, drifting with the wave motion or moving to an area of lower wave action (Friedlander et al., 2003; Fulton and Bellwood, 2005; Santin and Willis, 2007; Johansen et al., 2008; Heatwole and Fulton, 2013). However, for fish to remain in the water column and hold position to maintain access to resources (e.g. territory, nests, prey) requires constant swimming adjustments in the face of wave-induced flows (Liao, 2007; Webb et al., 2010; Heatwole and Fulton, 2013). The species tested represented four different swimming modes found among coral reef fishes (Table 1; Fulton, 2007). The caudal fin swimmers, also categorized as subcarangiform swimmers, were *Kuhlia* spp., the simultaneous pectoral–caudal fin (chaetodontiform) swimmers were *A. ocellaris*, the pectoral fin (labriform) swimmers were *C. strigosus*, and finally the dorsal–anal fin (balistiform) swimmers were *S. bursa* (Breder, 1926; Webb, 1998; Fulton, 2007). Both *Kuhlia* spp. and *A. ocellaris* employed BCF swimming, whereas *C. strigosus* and *S. bursa* swam exclusively with the median or paired fins (MPF swimming).

Pectoral fin beat frequencies and behavior with oscillatory swimming

The BCF swimmers were observed to turn around with swimming direction change, while the MPF swimmers often swam backwards during half the wave cycle rather than rotate the body, even at the highest wave intensities (Fig. 2; Movie 1). The BCF swimmers *Kuhlia* spp. and *A. ocellaris* turned around the vast majority of the time, and always above 0.2 Hz and 1.0 BL amplitude, in order to

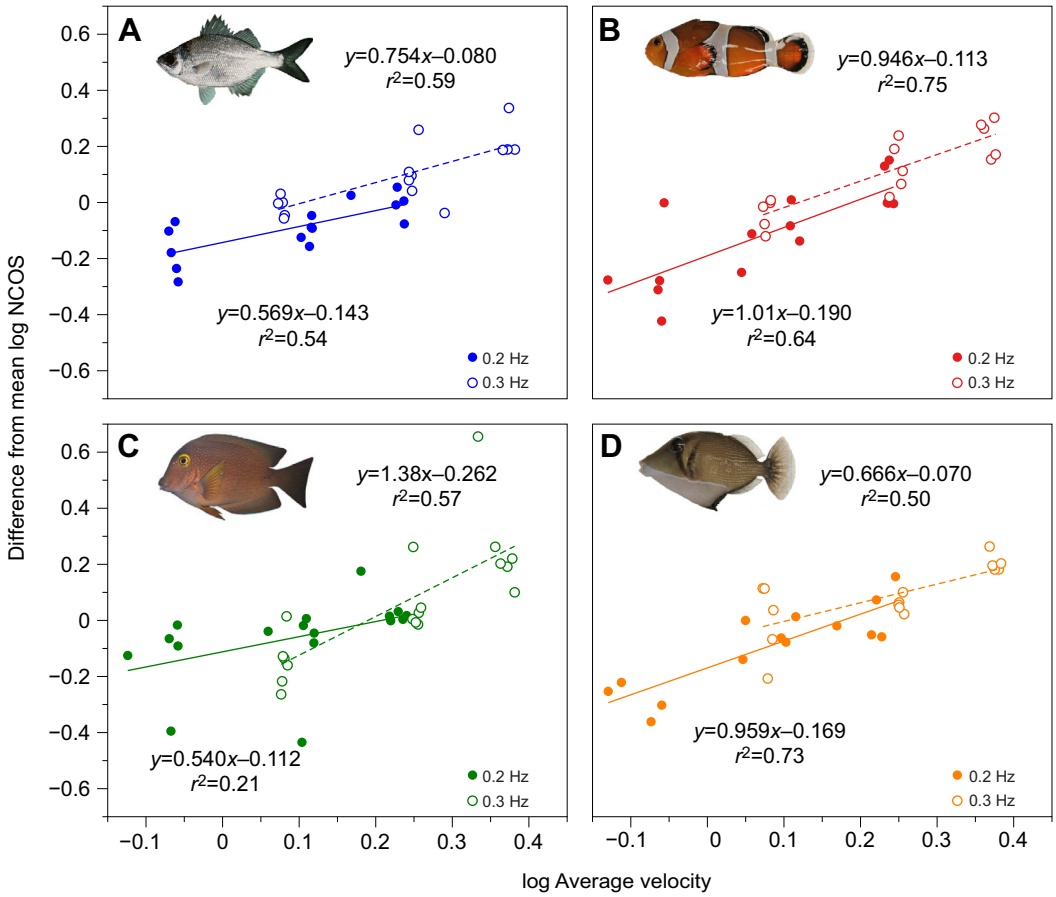

Fig. 6. Difference from average net cost of swimming (NCOS; mg O_2 kg^{-1} h^{-1}) as a function of average velocity (BL s^{-1}) at two frequencies of oscillatory swimming (0.2 and 0.3 Hz). Values were log transformed to linearize the relationship. (A) *Kuhlia* spp. (*n*=5, mean log NCOS=2.18), (B) *Amphiprion ocellaris* (*n*=5, mean log NCOS=2.32), (C) *Ctenochaetus strigosus* (*n*=6, mean log NCOS=2.16) and (D) *Sufflamen bursa* (*n*=5, mean log NCOS=2.38). Difference from mean log NCOS were calculated as the difference from the mean log NCOS for each individual fish. Lines indicate regressions for each frequency.

remain swimming forward (Fig. 2). Only at the lower wave intensities (average velocities <1.0 BL s^{-1}) were a few individuals observed to occasionally swim backwards. BCF swimming fishes are capable of swimming in reverse using backward sculling of the pectoral fins and may require recruitment of other fins as well (Webb and Fairchild, 2001; Flammang and Lauder, 2016). The pectoral-caudal swimmer *A. ocellaris* has large, rounded, low-aspect-ratio pectoral fins (0.8; Marcoux, 2016) but was the species observed to swim backwards the least. *Amphiprion ocellaris* showed overall increases in pectoral f_{FB} as wave intensity increased (Fig. 3). However, beat-to-beat f_{FB} did not show a consistent pattern of change over the cycle of velocity changes. *Amphiprion ocellaris* may change pectoral fin beat amplitudes or use of the caudal fin to accelerate and decelerate during each wave cycle. Both *Kuhlia* spp. and *A. ocellaris* have more elongated bodies compared with the MPF swimmers, and posterior shifting of the fish's center of mass may complicate stability issues when swimming backwards compared with the deeper-bodied *C. strigosus* and *S. bursa*, whose center of mass is closer to the propulsive fins (Weihs, 2002; Claverie and Wainwright, 2014; Webb and Weihs, 2015; Flammang and Lauder, 2016). For the BCF swimming species, the ability to swim backwards may be limited or highly inefficient compared with forward swimming.

Unlike the BCF swimmers, the two MPF swimmers, *C. strigosus* and *S. bursa*, were frequently observed to swim backwards with a direction change, rather than turn the body around (Fig. 2). All individuals were capable of turning around in the SWMR shuttle and were similar in body length to the BCF swimmers (Table 1; Movie 1), so we do not think space restrictions were responsible for this difference in behavior. In both species, the percentage of turning tended to increase with increasing wave frequency and amplitude (Fig. 2). The pectoral fin swimmer *C. strigosus* was most frequently observed to swim backwards and turned around with less than 30% of direction changes on average, even at the highest wave intensity (average velocity of 2.4 BL s^{-1}; Fig. 2). Backward swimming has been described previously for a pectoral fin swimmer, the freshwater angelfish (*Pterophyllum scalare*), up to steady velocities of 2.8 BL s^{-1} (Webb and Fairchild, 2001). Although there is limited research on fish swimming in reverse, Flammang and Lauder (2016) described fin kinematics of backward swimming in the bluegill sunfish (*Lepomis macrochirus*) as an orchestrated movement of multiple fins, individually recruited to counteract instability of yawing around the center of mass of the fish. *Lepomis macrochirus* must recruit not only the pectoral fins, but the dorsal and anal fins along with the caudal fin to produce thrust and simultaneously counteract small instabilities using the same fins. Although the study by Flammang and Lauder (2016) did not investigate the costs of swimming backwards, it could be hypothesized that the increased recruitment of muscle activity would increase metabolic rate, allocating more resources toward fin movement than while swimming forward, which is a much more stable endeavor (Tudorache et al., 2009; Flammang and Lauder, 2016).

Mean pectoral f_{FB} in *C. strigosus* increased with wave intensity during both forward and backward swimming (Fig. 4). However, average f_{FB} was significantly higher while swimming in reverse over most intensities, indicating that more fin beats were required to cover the same distance. Although not measured in the present study, it is likely that the pattern of pectoral fin motion also changes with backward swimming, as seen with *L. macrochirus*, and is not simply a reversal of forward swimming motions (Flammang and Lauder, 2016). The beat-to-beat changes over each half wave cycle revealed a consistent pattern for *C. strigosus* (Fig. 4). f_{FB} was high at the beginning as velocity increases, which would be expected as this was when acceleration was highest. f_{FB} then decreased as velocity peaked and acceleration was minimal, followed by an increase at the end of the cycle as velocity dropped to zero and the direction changed. This pattern was similar in both forward and backward swimming, although f_{FB} was higher at the beginning of each cycle when swimming backwards (Fig. 4). During the second half of the half-cycle, there is the possibility for energy savings if swimming velocity can decrease owing to passive coasting, or minimal fin deflections for braking (Fish and Lauder, 2017). However, fin beats continued throughout the cycle and the increase just before the direction change may indicate active braking motions or preparation for the direction change and acceleration. Although MPF swimming gaits are expected to aid in turning maneuvers, deep-bodied fishes with fewer vertebrae, as has been found in other acanthurids and tetraodontiforms, may have less flexible bodies and therefore require a greater physical space for turning and have lower agility (rate of turning), even if turning radius of the center of mass is very small (Brainerd and Patek, 1998; Gerstner, 1999; Walker, 2000; Webb and Fairchild, 2001). In addition, the high-aspect-ratio pectoral fins of *C. strigosus* (1.9; Marcoux, 2016) are thought to be less effective at low speeds and for maneuvering (Gerstner, 1999; Drucker and Lauder, 2000; Wainwright et al., 2002; Walker and Westneat, 2002), although this does not appear to hinder *C. strigosus* during the transient drops in velocity and backward swimming in an oscillatory, wave-surge swimming pattern.

Similarly, the dorsal–anal fin swimmer, *S. bursa*, was observed to swim in reverse rather than turn around most of the time (Fig. 2), further supporting the idea that MPF swimmers may employ different swimming behaviors in wave-driven action compared with BCF swimmers. The undulatory fins of median fin swimmers (dorsal and/or anal fins) can change amplitude, frequency, wavelength and direction of the wave propagating along the fin, which permits a high degree of maneuverability, stability and effective backward swimming (Blake, 2004; Sefati et al., 2013; Neveln et al., 2014; Youngerman et al., 2014).

Comparison of NCOS across species and swimming mode

Pectoral fin swimmers dominate coral reef areas with high wave-induced flows, which has been suggested to be due to greater swimming performance and efficiency with this swimming mode (Fulton et al., 2001, 2017; Fulton and Bellwood, 2005). However, the lowest overall increases in NCOS (metabolic rate above SMR) with wave intensity were seen for the caudal fin swimming *Kuhlia* spp. compared with the other three species studied (Table 2, Fig. 5). The lower NCOS in a BCF swimmer during oscillatory swimming compared with the MPF swimmers was unexpected, as BCF swimmers are generally considered more specialized for steady, high-speed swimming and higher power outputs for greater acceleration, while MPF swimming (e.g. pectoral or dorsal–anal fin swimming) is considered advantageous for greater maneuverability and stability at low speeds (Webb, 1984; Blake, 2004; Fish, 2010). Despite a presumed trade-off between fast, steady swimming ability and maneuverability, there is evidence that MPF swimming can be a more efficient form of steady locomotion, by keeping a rigid body to minimize body drag and reduce energy lost as a result of yawing motions (Lighthill and Blake, 1990; Webb, 1998; Blake, 2004; Bale et al., 2015). Studies of MPF swimmers during steady swimming indicate lower costs of transport and lower rates of increase in metabolic rate with increasing velocities (Webb, 1974; Gordon et al., 1989; Korsmeyer et al., 2002; Cannas et al., 2006; Jones et al., 2007; Kendall et al., 2007; Fulton et al., 2013a).

Comparisons of the energetic costs of maneuvering, however, have been lacking. The overall NCOS results of the present study also do not support the traditional model of trade-offs between BCF and MPF swimming efficiencies, as none of the MPF swimmers had lower energetic costs than the strict BCF swimmers while swimming in an oscillatory, station-holding pattern. BCF swimmers may reduce costs by using an intermittent swimming pattern of powered bursts and passive coasting with the body held rigid (Videler and Weihs, 1982). The caudal swimming *Kuhlia* spp. may likewise reduce NCOS if they can coast and minimize drag during the periods of deceleration during each wave cycle. It is also possible that the propensity for swimming backwards in the two MPF swimmers resulted in higher than expected costs, although it would be counterintuitive for the fish to choose to sustain a less economical swimming behavior.

In addition to swimming mode, the overall metabolic costs of swimming will be affected by a suite of traits, including differences in metabolic capacity, the characteristics of the muscle fibers, muscle–skeletal arrangements, body shape, and fin structure and kinematics, all of which complicate comparisons across species (Daniel, 1991; Drucker and Lauder, 2000; Korsmeyer and Dewar, 2001). Further studies will be needed to determine whether the differences in NCOS are simply a result of the particular species chosen in this study or a more general phenomenon related to these swimming modes.

Intraspecific changes in NCOS with wave frequency

In steady swimming, the NCOS in fishes increases with velocity following a power function, with ever increasing costs as velocity rises (Videler, 1993; Korsmeyer et al., 2002). Thus, as the peak velocity of oscillatory flows increase as a result of increases in wave amplitude or frequency, we would expect higher costs of swimming. In addition, bidirectional oscillatory swimming requires repeated accelerations and changes in direction not experienced by fish swimming in steady flows, which would be expected to add additional energetic costs (Webb et al., 2010; Heatwole and Fulton, 2013). With each half-wave cycle, velocity increased from zero to a peak velocity, requiring acceleration, followed by deceleration back to zero velocity and then a reversal in direction (Fig. 1). A previous study on the pectoral fin swimmer *Cymatogaster aggregata* measured energetic costs during steady swimming compared with cyclical variations in flow around a mean forward velocity (unidirectional wave surge, i.e. no change in flow direction; Roche et al., 2014). Cycles of 1.0 BL s^{-1} amplitude fluctuations in velocity increased energetic costs by 14% compared with estimates from steady swimming costs. This increase is presumably due to the added costs of accelerating and decelerating (Roche et al., 2014).

To examine the possible added costs of both accelerations and direction changes during bidirectional oscillatory swimming, we compared NCOS within each species at similar average velocities, but at different wave frequencies. In this study, similar average velocities were achieved between 1.2 and 1.7 BL s^{-1} at two different frequencies (0.2 Hz with A=1.5 to 2.0 BL, and 0.3 Hz with A=1.0 to 1.5 BL; Fig. 5). In addition, over this range of average velocities, the proportion of turning was comparable within each species at both frequencies (Fig. 2), so any differences cannot be attributed to changes in swimming behavior. With an increase from 0.2 to 0.3 Hz, the frequency of direction change increased from 12 per minute to 18, or a 50% increase, and average acceleration also increased by 50%, even as velocities remained the same.

For the caudal swimmers (*Kuhlia* spp.), the cost of swimming increased by 24% with an increase in wave frequency from 0.2 to 0.3 Hz at similar velocities (Fig. 6). This difference indicates the higher costs of acceleration, deceleration and maneuvering to change direction at the higher wave frequency in these species. The other species showed smaller changes in NCOS, on average, with increasing frequency of direction change. For the strict MPF swimmers, there was considerable overlap in NCOS between frequencies at the same average velocity (Fig. 6C,D), and the average change for *C. strigosus* was negligible (−3%). Although the difference in the effect of frequency on NCOS between *Kuhlia* spp. and *C. strigosus* did not reach statistical significance (P=0.16), the trend of a lower effect size compared with the BCF swimmers in both the dorsal–anal fin swimming *S. bursa* (+13%) and the pectoral fin swimming *C. strigosus* suggests that the added costs of swimming at higher wave frequencies may be lower with MPF swimming modes. The small sample size may have limited the ability to detect significance of these small differences in swimming costs, and further testing is warranted. Lower costs of direction changes could be a result of the greater maneuverability and stability afforded by the MPF swimming mode (Weihs, 2002; Blake, 2004), or be related to the behavior of swimming backwards to avoid turning in these species, although lower overall swimming costs were not found.

Conclusions

The SWMR apparatus proved to be an effective technique for inducing repeatable, bidirectional swimming behaviors in fishes. As the intensity of wave action increased in both frequency and amplitude, fishes attempting to station-hold were subject to significant increases in metabolic rate. Among the reef fishes with different swimming modes, the caudal swimming *Kuhlia* spp. showed lower overall swimming costs, but significant increases in NCOS with an increase in frequency of direction change, at similar swimming velocities. Although not conclusive, a trend of lower average effects of frequency on the two MPF swimmers (*C. strigosus* and *S. bursa*) suggests that they are adapted to reduce the added costs of station-holding as wave frequency increases, which would be consistent with field observations of the greater abundance of pectoral fin swimmers in reef habitats exposed to high wave-induced flows (Fulton, 2010). Future studies on additional species are needed to confirm whether these patterns of swimming costs are consistent within the different swimming modes. The MPF swimmers in this study revealed the behavioral flexibility of swimming backwards in these flows rather than turning the body around. As wave intensity increases, the percentage turning increases in the MPF swimmers, and subsequent studies should examine the costs of increasing frequency at higher average velocities (i.e. at greater wave amplitudes) that induce regular turning. In addition, direct comparisons of the costs of bidirectional, oscillatory swimming with steady swimming costs may better reveal any differences with swimming mode and the costs of direction changes. These types of studies will be needed to distinguish whether differences in added costs of acceleration and direction change in MPF swimmers are due directly to the rigid-body swimming mode, or the greater capacity to swim in reverse to avoid re-orienting themselves into the direction of flow.

Acknowledgements

Special thanks to Drs Chad Callan and Eric Vetter for insight and assistance with this project. Many thanks also to Corrie Wong and Stacia Goecke for contributions to this work in the lab, and Dr John Steffensen for helpful discussions. We also thank Dr K. David Hyrenbach for assistance with statistical analyses, and two anonymous reviewers for helpful comments that improved the manuscript. The data presented here were in part included in a Master's thesis by T.M.M.

Competing interests
The authors declare no competing or financial interests.

Author contributions
Conceptualization: T.M.M., K.E.K.; Methodology: K.E.K.; Software: K.E.K.; Validation: T.M.M., K.E.K.; Formal analysis: T.M.M., K.E.K.; Investigation: T.M.M.; Resources: K.E.K.; Data curation: T.M.M., K.E.K.; Writing - original draft: T.M.M.; Writing - review & editing: T.M.M., K.E.K.; Visualization: T.M.M., K.E.K.; Supervision: K.E.K.; Project administration: K.E.K.; Funding acquisition: K.E.K.

Funding
This work was supported by the College of Natural and Computational Sciences, Hawaii Pacific University.

Supplementary information
Supplementary information available online at
http://jeb.biologists.org/lookup/doi/10.1242/jeb.191791.supplemental

References

Arnold, G. P. (1974). Rheotropism in fishes. *Biol. Rev. Camb. Philos. Soc.* **49**, 515-576.
Bale, R., Neveln, I. D., Bhalla, A. P. S., MacIver, M. A. and Patankar, N. A. (2015). Convergent evolution of mechanically optimal locomotion in aquatic invertebrates and vertebrates. *PLoS Biol.* **13**, e1002123.
Bellwood, D. R. and Wainwright, P. C. (2001). Locomotion in labrid fishes: implications for habitat use and cross-shelf biogeography on the Great Barrier Reef. *Coral Reefs* **20**, 139-150.
Blake, R. W. (2004). Fish functional design and swimming performance. *J. Fish Biol.* **65**, 1193-1222.
Brainerd, E. L. and Patek, S. N. (1998). Vertebral column morphology, C-start curvature, and the evolution of mechanical defenses in tetraodontiform fishes. *Copeia* **1998**, 971-984.
Breder, C. M. (1926). The locomotion of fishes. *Zoologica (N. Y.)* **4**, 159-297.
Cannas, M., Schaefer, J., Domenici, P. and Steffensen, J. F. (2006). Gait transition and oxygen consumption in swimming striped surfperch *Embiotoca lateralis* Agassiz. *J. Fish Biol.* **69**, 1612-1625.
Chabot, D., Steffensen, J. F. and Farrell, A. P. (2016). The determination of standard metabolic rate in fishes. *J. Fish Biol.* **88**, 81-121.
Clark, T. D., Sandblom, E. and Jutfelt, F. (2013). Aerobic scope measurements of fishes in an era of climate change: respirometry, relevance and recommendations. *J. Exp. Biol.* **216**, 2771-2782.
Clarke, R. D., Finelli, C. M. and Buskey, E. J. (2009). Water flow controls distribution and feeding behavior of two co-occurring coral reef fishes: II. Laboratory experiments. *Coral Reefs* **28**, 475-488.
Claverie, T. and Wainwright, P. C. (2014). A morphospace for reef fishes: elongation is the dominant axis of body shape evolution. *PLoS ONE* **9**, e112732.
Constantin, A. and Villari, G. (2008). Particle trajectories in linear water waves. *J. Math. Fluid Mech.* **10**, 1-18.
Daniel, T. (1991). Efficiency in aquatic locomotion: limitations from single cells to animals. In *Efficiency and Economy in Animal Physiology* (ed. R. W. Blake), pp. 83-95. Cambridge: Cambridge University Press.
Denny, M. W. (2006). Ocean waves, nearshore ecology, and natural selection. *Aquat. Ecol.* **40**, 439-461.
Denny, M. W. and Gaylord, B. (2010). Marine ecomechanics. *Ann. Rev. Mar. Sci.* **2**, 89-114.
Domenici, P. (2010). Escape responses in fish: kinematics, performance and behavior. In *Fish Locomotion: An Etho-Ecological Perspective* (ed. P. Domenici and B. G. Kapoor), pp. 123-170. Enfield, NH: Science Publishers.
Drucker, E. G. and Lauder, G. V. (2000). A hydrodynamic analysis of fish swimming speed: wake structure and locomotor force in slow and fast labriform swimmers. *J. Exp. Biol.* **203**, 2379-2393.
Fish, F. E. (2010). Swimming strategies for energy economy. In *Fish Locomotion: an Eco-Ethological Perspective* (ed. P. Domenici and B. G. Kapoor), pp. 90-122. Enfield, NH: Science Publishers.
Fish, F. E. and Hoffman, J. L. (2015). Stability design and response to waves by batoids. *Integr. Comp. Biol.* **55**, 648-661.
Fish, F. E. and Lauder, G. V. (2017). Control surfaces of aquatic vertebrates: active and passive design and function. *J. Exp. Biol.* **220**, 4351-4363.
Flammang, B. E. and Lauder, G. V. (2016). Functional morphology and hydrodynamics of backward swimming in bluegill sunfish, *Lepomis macrochirus*. *Zoology* **119**, 414-420.
Friedlander, A. M., Brown, E. K., Jokiel, P. L., Smith, W. R. and Rodgers, K. S. (2003). Effects of habitat, wave exposure, and marine protected area status on coral reef fish assemblages in the Hawaiian archipelago. *Coral Reefs* **22**, 291-305.
Fulton, C. J. (2007). Swimming speed performance in coral reef fishes: field validations reveal distinct functional groups. *Coral Reefs* **26**, 217-228.
Fulton, C. J. (2010). The role of swimming in reef fish ecology. In *Fish Locomotion: an Eco-Ethological Perspective* (ed. P. Domenici and B. G. Kapoor), pp. 374-406. Enfield, NH: Science Publishers.
Fulton, C. J. and Bellwood, D. R. (2005). Wave-induced water motion and the functional implications for coral reef fish assemblages. *Limnol. Oceanogr.* **50**, 255-264.
Fulton, C. J., Bellwood, D. R. and Wainwright, P. C. (2001). The relationship between swimming ability and habitat use in wrasses (Labridae). *Mar. Biol.* **139**, 25-33.
Fulton, C. J., Bellwood, D. R. and Wainwright, P. C. (2005). Wave energy and swimming performance shape coral reef fish assemblages. *Proc. R. Soc. B* **272**, 827-832.
Fulton, C. J., Johansen, J. L. and Steffensen, J. F. (2013a). Energetic extremes in aquatic locomotion by coral reef fishes. *PLoS ONE* **8**, e54033.
Fulton, C. J., Binning, S. A., Wainwright, P. C. and Bellwood, D. R. (2013b). Wave-induced abiotic stress shapes phenotypic diversity in a coral reef fish across a geographical cline. *Coral Reefs* **32**, 685-689.
Fulton, C. J., Wainwright, P. C., Hoey, A. S. and Bellwood, D. R. (2017). Global ecological success of *Thalassoma* fishes in extreme coral reef habitats. *Ecol. Evol.* **7**, 466-472.
Gerstner, C. L. (1999). Maneuverability of four species of coral-reef fish that differ in body and pectoral-fin morphology. *Can. J. Zool.* **77**, 1102-1110.
Gordon, M. S., Chin, H. G. and Vojkovich, M. (1989). Energetics of swimming in fishes using different methods of locomotion: I. Labriform swimmers. *Fish Physiol. Biochem.* **6**, 341-352.
Harden Jones, F. R. (1963). The reaction of fish to moving backgrounds. *J. Exp. Biol.* **40**, 437-446.
Heatwole, S. J. and Fulton, C. J. (2013). Behavioural flexibility in reef fishes responding to a rapidly changing wave environment. *Mar. Biol.* **160**, 677-689.
Johansen, J. L., Bellwood, D. R. and Fulton, C. J. (2008). Coral reef fishes exploit flow refuges in high-flow habitats. *Mar. Ecol. Prog. Ser.* **360**, 219-226.
Jones, E. A., Lucey, K. S. and Ellerby, D. J. (2007). Efficiency of labriform swimming in the bluegill sunfish (*Lepomis macrochirus*). *J. Exp. Biol.* **210**, 3422-3429.
Kendall, J. L., Lucey, K. S., Jones, E. A., Wang, J. and Ellerby, D. J. (2007). Mechanical and energetic factors underlying gait transitions in bluegill sunfish (*Lepomis macrochirus*). *J. Exp. Biol.* **210**, 4265-4271.
Korsmeyer, K. E. and Dewar, H. (2001). Tuna metabolism and energetics. In *Tuna: Physiology, Ecology and Evolution* (ed. B. A. Block and E. D. Stevens), pp. 35-78. San Diego: Academic Press.
Korsmeyer, K. E., Steffensen, J. F. and Herskin, J. (2002). Energetics of median and paired fin swimming, body and caudal fin swimming, and gait transition in parrotfish (*Scarus schlegeli*) and triggerfish (*Rhinecanthus aculeatus*). *J. Exp. Biol.* **205**, 1253-1263.
Langerhans, R. B. (2008). Predictability of phenotypic differentiation across flow regimes in fishes. *Integr. Comp. Biol.* **48**, 750-768.
Langerhans, R. B. and Reznick, D. N. (2010). Ecology and evolution of swimming performance in fishes: predicting evolution with biomechanics. In *Fish Locomotion: an Eco-Ethological Perspective* (ed. P. Domenici and B. G. Kapoor), pp. 200-248. Enfield, NH: Science Publishers.
Lauder, G. V. and Liem, K. F. (1983). The evolution and interrelationships of the actinopterygian fishes. *Bull. Mus. Comp. Zool.* **150**, 95-197.
Liao, J. C. (2007). A review of fish swimming mechanics and behaviour in altered flows. *Philos. Trans. R. Soc. Lond. B. Biol. Sci.* **362**, 1973-1993.
Lighthill, J. and Blake, R. (1990). Biofluiddynamics of balistiform and gymnotiform locomotion. Part 1. Biological background, and analysis by elongated-body theory. *J. Fluid Mech.* **212**, 183-207.
Lowe, R. J., Falter, J. L., Bandet, M. D., Pawlak, G., Atkinson, M. J., Monismith, S. G. and Koseff, J. R. (2005). Spectral wave dissipation over a barrier reef. *J. Geophys. Res.* **110**, C04001.
Madin, J. S., Black, K. P. and Connolly, S. R. (2006). Scaling water motion on coral reefs: from regional to organismal scales. *Coral Reefs* **25**, 635-644.
Marcoux, T. M. (2016). Wave-induced stress and its effects on coral reef fish swimming performance and energetics. *MSc thesis*, Hawaii Pacific University, Honolulu, HI.
Meijering, E., Dzyubachyk, O. and Smal, I. (2012). Methods for cell and particle tracking. *Methods Enzymol.* **504**, 183-200.
Moberg, F. and Folke, C. (1999). Ecological goods and services of coral reef ecosystems. *Ecol. Econ.* **29**, 215-233.
Neveln, I. D., Bale, R., Bhalla, A. P. S., Curet, O. M., Patankar, N. A. and MacIver, M. A. (2014). Undulating fins produce off-axis thrust and flow structures. *J. Exp. Biol.* **217**, 201-213.
Pink, J. R. and Fulton, C. J. (2014). Right tools for the task: intraspecific modality in the swimming behaviour of coral reef fishes. *Mar. Biol.* **161**, 1103-1111.
Price, S. A., Holzman, R., Near, T. J. and Wainwright, P. C. (2011). Coral reefs promote the evolution of morphological diversity and ecological novelty in labrid fishes. *Ecol. Lett.* **14**, 462-469.
Randall, J. E. and Randall, H. A. (2001). Review of the fishes of the genus *Kuhlia* (Perciformes: Kuhliidae) of the Central Pacific. *Pac. Sci.* **55**, 227-256.

Roche, D. G., Taylor, M. K., Binning, S. A., Johansen, J. L., Domenici, P. and Steffensen, J. F. (2014). Unsteady flow affects swimming energetics in a labriform fish (*Cymatogaster aggregata*). *J. Exp. Biol.* **217**, 414-422.
Santin, S. and Willis, T. J. (2007). Direct versus indirect effects of wave exposure as a structuring force on temperate cryptobenthic fish assemblages. *Mar. Biol.* **151**, 1683-1694.
Sefati, S., Neveln, I. D., Roth, E., Mitchell, T. R. T., Snyder, J. B., Maciver, M. A., Fortune, E. S. and Cowan, N. J. (2013). Mutually opposing forces during locomotion can eliminate the tradeoff between maneuverability and stability. *Proc. Natl. Acad. Sci. USA* **110**, 18798-18803.
Steffensen, J. F., Bushnell, P. G. and Schurmann, H. (1994). Oxygen consumption in four species of teleosts from Greenland: no evidence of metabolic cold adaptation. *Polar Biol.* **14**, 49-54.
Svendsen, J. C., Tudorache, C., Jordan, A. D., Steffensen, J. F., Aarestrup, K. and Domenici, P. (2010). Partition of aerobic and anaerobic swimming costs related to gait transitions in a labriform swimmer. *J. Exp. Biol.* **213**, 2177-2183.
Svendsen, M. B., Bushnell, P. G. and Steffensen, J. F. (2016). Design and setup of intermittent-flow respirometry system for aquatic organisms. *J. Fish Biol.* **88**, 26-50.
Tudorache, C., Jordan, A. D., Svendsen, J. C., Domenici, P., DeBoeck, G. and Steffensen, J. F. (2009). Pectoral fin beat frequency predicts oxygen consumption during spontaneous activity in a labriform swimming fish (*Embiotoca lateralis*). *Environ. Biol. Fishes* **84**, 121-127.
Tudorache, C., de Boeck, G. and Claireaux, G. (2013). Forced and preferred swimming speeds of fish: a methodological approach. In *Swimming Physiology of Fish* (ed. A. P. Palstra and J. V. Planas), pp. 81-108. Berlin: Springer-Verlag.
Videler, J. J. (1993). *Fish Swimming*. New York: Chapman and Hall.
Videler, J. J. and Weihs, D. (1982). Energetic advantages of burst-and-coast swimming of fish at high speeds. *J. Exp. Biol.* **97**, 169-178.
Vogel, S. (1994). *Life in Moving Fluids: The Physical Biology of Flow*. Princeton, NJ: Princeton University Press.
Wainwright, P., Bellwood, D. R. and Westneat, M. W. (2002). Ecomorphology of locomotion in labrid fishes. *Environ. Biol. Fishes* **65**, 47-62.
Walker, J. A. (2000). Does a rigid body limit maneuverability? *J. Exp. Biol.* **203**, 3391-3396.
Walker, J. A. and Westneat, M. W. (2002). Performance limits of labriform propulsion and correlates with fin shape and motion. *J. Exp. Biol.* **205**, 177-187.
Webb, P. W. (1974). Efficiency of pectoral-fin propulsion of *Cymatogaster aggregata*. In *Swimming and Flying in Nature*, Vol. 2 (ed. T. Y.-T. Wu, C. J. Brokaw and C. Brennen), pp. 573-584. New York: Plenum Press.
Webb, P. W. (1984). Body form, locomotion and foraging in aquatic vertebrates. *Am. Zool.* **24**, 107-120.
Webb, P. W. (1994). The biology of fish swimming. In *Mechanics and Physiology of Animal Swimming* (ed. L. Maddock, Q. Bone and J. M. V. Rayner), pp. 45-62. Cambridge: Cambridge University Press.
Webb, P. W. (1998). Swimming. In *The Physiology of Fishes* (ed. D. H. Evans), pp. 3-24. Boca Raton: CRC Press.
Webb, P. W. and Fairchild, A. G. (2001). Performance and maneuverability of three species of teleostean fishes. *Can. J. Zool.* **79**, 1866-1877.
Webb, P. W. and Weihs, D. (2015). Stability versus maneuvering: challenges for stability during swimming by fishes. *Integr. Comp. Biol.* **55**, 753-764.
Webb, P. W., Cotel, A. and Meadows, L. A. (2010). Waves and eddies: effects on fish behavior and habitat distribution. In *Fish Locomotion: an Eco-Ethological Perspective* (ed. P. Domenici and B. G. Kapoor), pp. 1-39. Enfield, NH: Science Publishers.
Weihs, D. (2002). Stability versus maneuverability in aquatic locomotion. *Integr. Comp. Biol.* **42**, 127-134.
West, B. T., Welch, K. B. and Galecki, A. T. (2014). *Linear Mixed Models. A Practical Guide Using Statistical Software*. Boca Raton, FL: Chapman and Hall/CRC.
Youngerman, E. D., Flammang, B. E. and Lauder, G. V. (2014). Locomotion of free-swimming ghost knifefish: anal fin kinematics during four behaviors. *Zoology* **117**, 337-348.